Time-dependent *R*-matrix calculations for multiphoton ionization of argon atoms in strong laser pulses

Xiaoxu Guan,[1] C. J. Noble,[1,*] O. Zatsarinny,[1] K. Bartschat,[1] and B. I. Schneider[2]
[1]*Department of Physics and Astronomy, Drake University, Des Moines, Iowa 50311, USA*
[2]*Physics Division, National Science Foundation, Arlington, Virgina 22230, USA*
(Received 9 September 2008; published 5 November 2008)

A recently developed [Guan *et al.*, Phys. Rev. A **76**, 053411 (2007)] general *ab initio* and nonperturbative method to solve the time-dependent Schrödinger equation (TDSE) for the interaction of a strong attosecond laser pulse with a general atom is applied to multiphoton ionization of argon atoms. The field-free Hamiltonian and the dipole matrices are generated using a flexible *B*-spline *R*-matrix method, which allows for the use of nonorthogonal sets of one-electron orbitals. The solution of the TDSE is propagated in time using the Arnoldi-Lanczos method. The effects of the pulse length and the laser intensity on the ionization rate for different photon energies are analyzed. In the long-pulse regime, good agreement with predictions from *R*-matrix Floquet calculations is achieved.

DOI: 10.1103/PhysRevA.78.053402 PACS number(s): 32.80.Fb

I. INTRODUCTION

In a recent paper [1], we described a general *ab initio* and nonperturbative method to solve the time-dependent Schrödinger equation (TDSE) for the interaction of a strong attosecond laser pulse with a general atom, i.e., beyond the models of quasi-one-electron or quasi-two-electron targets. The critical ingredients of our time-dependent *B*-spline *R*-matrix (TDBSR) approach are field-free Hamiltonian and dipole matrices, which are generated using a flexible *B*-spline *R*-matrix method [2], followed by the propagation of the TDSE using the Arnoldi-Lanczos method [3,4]. The latter propagation scheme avoids the diagonalization of any large matrices. The method was illustrated by an application to the multiphoton excitation and ionization of Ne atoms, and good agreement with *R*-matrix Floquet results for the generalized cross sections for two-photon ionization was achieved.

As pointed out earlier (see [1], and references therein), the rapid progress in the development of ultrashort and ultraintense light sources is providing a window to study the details of electron interactions in atoms, molecules, plasmas, and solids on an attosecond time scale. These capabilities promise a revolution in our microscopic knowledge and understanding of matter [5,6]. There is no doubt that highly challenging experiments such as those reported in [7,8] will benefit tremendously from theoretical support in order to reap the maximum profits from the enormous resources being invested in the experimental facilities.

The ingredients of an appropriate theoretical and computational formulation require an accurate and efficient generation of the Hamiltonian and the electron-field interaction matrix elements, as well as an optimal approach to propagate the TDSE in real time. There have been numerous calculations for two-electron systems such as He and H_2. (A partial list of references can be found in Guan *et al.* [9].) While these investigations emphasize the important role of two-electron systems in studying electron-electron correlation in the presence of a strong laser field, in its presumably purest form, experiments with He atoms are difficult and other noble gases, such as Ne and Ar, are often favored by the experimental community.

Fully *ab initio* theoretical approaches, which are applicable to complex targets beyond (quasi) two-electron systems, are still rare. For (infinitely) long interaction times, the *R*-matrix Floquet ansatz [11] has been highly successful. A critical ingredient of this method is the general atomic *R*-matrix method developed over many years by Burke and collaborators in Belfast. A modification of the method, allowing for relatively long though finite-length pulses was described by Plummer and Noble [12]. Recently, a time-dependent formulation [13] of this method was applied to short-pulse laser interactions with Ar [14].

In this paper, we apply our TDBSR method to the laser-Ar problem as well. Since the publication of our previous paper [1], we have gained additional insight into the numerical intricacies of the problem and will describe some important algorithmic improvements in Sec. II. Our approach now enables us to perform calculations at significantly longer wavelengths and, consequently, to treat more photons while, at the same time, increasing the number of coupled channels. We can also use a significantly larger box size, thereby eliminating the need for absorption potentials, which can be problematic in the extraction of physically meaningful results. Specifically, we will present in Sec. III results for two-photon, three-photon, and five-photon ionization of Ar atoms by laser pulses of durations between 10 and 60 optical cycles (o.c.) and wavelengths between 88 and 390 nm. Finally, Sec. IV gives our conclusions and an outlook to the future.

Unless specified otherwise, atomic units (a.u.) are used throughout this manuscript.

II. NUMERICAL METHOD

A detailed description of the TDBSR method has been given by Guan *et al.* [1] and hence will not be repeated here.

*Permanent address: Computational Science and Engineering Department, Daresbury Laboratory, Warrington WA4 4AD, UK.

Instead, we briefly summarize the basic equations and then concentrate on essential improvements achieved during the past year.

A. TDBSR approach

The TDSE for the N-electron wave function $\Psi(\mathbf{r}_1,\ldots,\mathbf{r}_N;t)$ of the present problem is given by

$$i\frac{\partial}{\partial t}\Psi(\mathbf{r}_1,\ldots,\mathbf{r}_N;t) = [H_0(\mathbf{r}_1,\ldots,\mathbf{r}_N) + V(\mathbf{r}_1,\ldots,\mathbf{r}_N;t)]\Psi(\mathbf{r}_1,\ldots,\mathbf{r}_N;t), \tag{1}$$

where $H_0(\mathbf{r}_1,\ldots,\mathbf{r}_N)$ is the field-free Hamiltonian containing the sum of the kinetic energy of the N electrons, their potential energy in the field of the nucleus (we assume an infinite nuclear mass), and their mutual Coulomb repulsion, while $V(\mathbf{r}_1,\ldots,\mathbf{r}_N;t)$ represents the interaction of the electrons with the electromagnetic field. For simplicity of notation, we omit the spin coordinates of the electrons.

We expand the wave function as

$$\Psi(\mathbf{r}_1,\ldots,\mathbf{r}_N;t) = \sum_q C_q(t)\Phi_q(\mathbf{r}_1,\ldots,\mathbf{r}_N). \tag{2}$$

Here $\Phi_q(\mathbf{r}_1,\ldots,\mathbf{r}_N)$ are a known set of N-electron states formed from appropriately symmetrized products of atomic orbitals.

The interaction of the atomic electrons with the time-dependent electric potential, in the length form of the electric dipole approximation, is given by

$$V(\mathbf{r}_1,\ldots,\mathbf{r}_N;t) = \sum_{i=1}^{N}\mathbf{E}(t)\cdot\mathbf{r}_i, \tag{3}$$

where $\mathbf{E}(t)$ is the electric field. This form has been used for the calculations in this paper.

When the expansion in Eq. (2) is inserted into the Schrödinger equation, we obtain

$$i\mathbf{S}\frac{\partial}{\partial t}\mathbf{C}(t) = [\mathbf{H}_0 + E(t)\mathbf{D}]\mathbf{C}(t), \tag{4}$$

where $\mathbf{S}$ is the overlap matrix of the basis functions, $\mathbf{H}_0$ and $\mathbf{D}$ are matrix representations of the field-free Hamiltonian and the dipole coupling matrices, and $\mathbf{C}(t)$ is the time-dependent vector of coefficients in Eq. (2). Since we are initially interested in excitation and single ionization of the target atom by the laser pulse, the field-free Hamiltonian must also contain a sufficient number of singly excited bound states as well as the continuum states representing electron scattering from the residual ion. As a method developed to treat exactly such problems, the time-independent B-spline R-matrix (BSR) approach [2] is particularly suitable to represent these states.

A significant advantage of the BSR method in the calculation of both bound and continuum states is the possibility of employing nonorthogonal sets of atomic orbitals for different target states, thereby omitting the need for pseudo-orbitals to account for the strong configuration or even term dependence that exists in many complex targets, with the noble gases being a prime example. This flexibility allows for optimization procedures that are tailored to the individual neutral, ionic, and continuum orbitals. As a result, accurate structure and collision calculations are possible with relatively small multiconfiguration expansions. The price to pay, at least initially, is the representation of the field-free Hamiltonian and the dipole matrices in a nonorthogonal basis. In standard applications of the BSR method, this leads to a generalized eigenvalue problem, for which effective computer packages are commonly available.

In our previous work [1], we described two methods of combining the BSR method with a highly efficient Arnoldi-Lanczos propagation scheme. In the first one, we diagonalized the overlap matrix $\mathbf{S}$ and transformed the problem back to an orthogonal basis before applying the standard propagation scheme [3,4]. Alternatively, the propagation can be done more directly in the nonorthogonal basis. This only requires a Cholesky decomposition of $\mathbf{S}$, but some additional operations at every time step. A third approach, which involves a transformation into the eigenbasis of the problem, was used in the present work and will be described in the next subsection. Depending on the size of the matrices to be handled, even more sophisticated methods may be required that do not require the diagonalization or decomposition of large matrices [15].

B. Transformation to the eigenbasis

As will be seen below, an important aspect of the calculation is the energy spectrum of the field-free Hamiltonian. We require a time propagation scheme, which contains all the important physics associated with the laser-driven system while at the same time being highly efficient and stable. Using B splines in configuration space, we found that the highest eigenvalue ($E_{\max}$) of the field-free Hamiltonian in a given L symmetry could become as large as 10^6 a.u. for the present problem, as a consequence of the closely spaced mesh of knots required near the origin. If such eigenvalues and the corresponding underlying basis functions were kept in the time propagation scheme, very small time steps ($\Delta t_{\min} \leqslant 2\pi/E_{\max}$) would generally be required to keep the propagation scheme stable. Typically laser frequencies are of the order of 1 a.u. ($\approx$27 eV), i.e., the laser-induced physics varies on a much coarser time scale. As a consequence, we are propagating target pseudostates in the expansion with energies of several hundred atomic units or more, which are very unlikely to be populated during the interaction, assuming we are in the target ground state, i.e., in the lowest eigenstate of the field-free Hamiltonian, at $t=0$.

A straightforward way to address this problem is to solve the field-free generalized eigenvalue problem

$$\mathbf{H}_0\mathbf{v}^L = E\mathbf{S}\mathbf{v}^L \tag{5}$$

for each symmetry with total orbital angular momentum L. (Recall that, due to the dipole selection rules and a ^1S initial state, we only need to include the symmetries ^1S, $^1P^o$, ^1D, $^1F^o$,....) This gives us the eigenbasis of column vectors $\mathbf{v}_n^L$, $n=1,2,\ldots,n_r^L$, with eigenvalues E_n^L, where n_r^L is the rank of the matrix for this particular symmetry.

Having obtained this eigenbasis, we now define the transformation matrix

$$\mathbf{A}^L \equiv (\mathbf{v}_1^L, \mathbf{v}_2^L, \ldots, \mathbf{v}_c^L), \tag{6}$$

i.e., we drop the eigenvectors corresponding to eigenvalues $E_n^L > E_c$. We then transform the field-free Hamiltonian and the dipole matrices coupling L and L' according to

$$\tilde{\mathbf{H}}_0^L \equiv (\mathbf{A}^L)^T \mathbf{H}_0^L \mathbf{A}^L, \tag{7}$$

$$\tilde{\mathbf{D}}^{LL'} \equiv (\mathbf{A}^L)^T \mathbf{D}^{LL'} \mathbf{A}^{L'}. \tag{8}$$

Here the superscript "T" indicates the transposed matrix. As a result, the field-free Hamiltonian is now diagonal with the energy eigenvalues $E_n^L < E_c$ as the diagonal elements, while the dipole matrices are represented in the truncated eigenbasis. The initial state in this representation is the column vector (1,0,0,…,0), and the extraction of survival, excitation, and ionization probabilities is straightforward. After the time propagation, the first element of the vector squared yields the survival probability of the ground state, the sum of the squares of all other coefficients corresponding to eigenstates below the ionization threshold represents excitation, and the sum of the squares of the remaining coefficients corresponds to ionization. Also, one can easily extract the information for particular partial-wave symmetries. Finally, after the transformation the problem is orthogonal in the truncated eigenbasis, and hence we can use the standard Arnoldi-Lanczos time-propagation scheme. The essential result of this analysis is a noticeably reduced number of required time steps per optical cycle, without any loss of physical information or precision.

In the present work, the "cut" (c) energy was chosen as $E_c = 10$ a.u., i.e., 537 a.u. above the ground state of neutral argon, and tests were performed to ensure that the final results did not depend (beyond the thickness of the lines in the figures below) on this value. Note, however, that the present calculations were performed in the length gauge of the dipole operator. Further checks would be required if the velocity gauge were to be used. This gauge is advantageous for very intense fields, but it emphasizes the spatial region near the nucleus, which may be sensitive to the omission of high-energy excitations [14].

C. Extraction of multiphoton generalized cross section

Once we have obtained the time-dependent wave function of the laser-driven system, we need to extract the physical quantities, such as the multiphoton generalized cross section or ionization rate. A meaningful N-photon generalized cross section (N being the number of photons absorbed) may be defined and extracted from the solution to the TDSE, as long as proper care is taken regarding the intensity, duration, and shape of the laser pulse. If perturbation theory is valid, this cross section can also be calculated using time-independent methods (infinitely long "pulses"). In practical calculations, a small dependence of the extracted cross section on these parameters can occur, but this can be controlled by suitably choosing the intensity and duration of the laser pulse. As long as the peak intensity (I_0) of the applied laser pulse is relatively weak, it is possible to extract the N-photon generalized cross section as

$$\sigma^{(N)} = \left(\frac{\omega}{I_0}\right)^N \frac{P_{\text{ion}}}{T_{\text{eff}}^{(N)}}, \tag{9}$$

where P_{ion} denotes the ionization yield at the end of the pulse and the effective interaction time $T_{\text{eff}}^{(N)}$ is defined through

$$T_{\text{eff}}^{(N)} = \int_0^\tau f^{2N}(t)dt. \tag{10}$$

Here $f(t)$ is the pulse shape function of the temporal laser field. According to Eq. (9), the generalized cross section for an N-photon process is defined in units of $\text{cm}^{2N}\,\text{s}^{N-1}$. As shown recently by Guan *et al.* [9] and by Feist *et al.* [10], this proper definition of the effective interaction time resolves many of the discrepancies seen in otherwise very similar calculations for two-photon double ionization of helium. If necessary, even the depletion of the initial state can be properly accounted for (see Eqs. (23) and (25) of Guan *et al.* [9]). This depletion is unavoidable, particularly for long pulses. Note, however, that its occurrence alone does not imply that perturbation theory becomes an invalid tool for treating the problem. We emphasize that the above procedure for extracting multiphoton cross sections is general and valid for both resonant and nonresonant multiphoton processes. For nonresonant ionization, the survival probability decreases exponentially for long times. This provides a way to extract the ionization rate through the exponent. If resonances are present, however, the ionization decay of the system is not purely exponential, and thus any ionization rate or cross section estimated in this way may be subject to some uncertainty [16].

D. Application to argon

In this work, we employ a three-state close-coupling expansion to describe the scattering of the ejected electron from the residual Ar^+ ion. Specifically, we include the $(3s^2 3p^5)^2 P^o$, $(3s 3p^6)^2 S$, and $(3s^2 3p^4 3d)^2 S$ states of Ar^+.

As pointed out by Burke and Taylor [17] more than three decades ago, an accurate description of these states is by no means trivial. There is a strong configuration dependence in the $3s$ and $3p$ orbitals for the ionic states, as well as for the initial $(3s^2 3p^6)^1 S$ bound state. If only a single set of orthogonal one-electron orbitals are employed in the calculation, the inclusion of a large set of additional configurations built using a suitable set of pseudo-orbitals [14,17] is necessary to obtain numerically accurate results.

In the present BSR method, we employ a different, fully relaxed and optimized $3s$ and $3p$ orbital for each of the principal configurations mentioned above. The Ar^+ ionic states were calculated using the MCHF approach [18], considering all single and double excitations of the $3s$ and $3p$ electrons into the $\bar{4}l$ ($l=0-3$) correlated orbitals. In the final expansions, however, we only kept configurations with coefficients greater than 0.02. We observed extremely strong configuration mixing between the $(3s 3p^6)^2 S$ and $(3s^2 3p^4 3d)^2 S$ ionic

states and consequently retained both channels in the final close-coupling expansion.

The radial wave functions of the outer electron were expanded in terms of a set of 561 *B*-splines of order eight, using a semiexponential distribution of knots that allowed for a numerically accurate description close to and far away from the nucleus (up to $r_{max}=500$ a.u.).

Even with the flexibility available in the BSR approach, an accurate description of the $(3s^23p^6)^1S$ initial state of neutral Ar remains a challenge. Consequently, we added 17 bound configurations to the close-coupling expansion for the ^1S symmetry. These configurations were obtained in separate MCHF calculations, using the same general approach as for the ionic states described above.

We obtained the absolute energies of the $\mathrm{Ar}(3s^23p^6)^1S$ initial state and the $\mathrm{Ar}^+(3s^23p^5)^2P^o$ ionic ground state as −527.015 55 and −526.437 50 a.u., respectively. These values correspond to an ionization energy of 15.73 eV while the experimental value is 15.76 eV [19]. The thresholds for ionization plus excitation to the other two ionic states in our model were obtained as 29.19 and 38.72 eV, respectively. The positions of these excited ionic states, as well as the low-lying excited states of neutral Ar, are crucial in determining the resonance phenomena predicted in the multiphoton ionization process (see below). Given the complexity of the target and the fact that we need to describe the interaction of the ejected electron with the residual ion in a collision setting rather than performing a structure-only calculation, we believe that the present structure description is excellent and more than sufficient for the problem of interest.

Before presenting the results of the generalized cross sections and ionization rates in the next section, a few remarks about the basis and the laser parameters are in order. In our previous work treating the neon atom in a strong laser pulse, we confined the system to a box of 100 a.u. With this size of the computational grid it was necessary to introduce an absorbing potential to avoid artificial reflection from the box boundary. In the present work, we were able to extend the box size to 500 a.u. For the pulses used in the calculation, we were able to avoid the introduction of an absorbing potential and to thus eliminate any lingering numerical issues associated with its presence. Reflection from the boundary is simply not an issue for this size box and these pulse durations. Finally, the calculations were done at laser wavelengths ranging from 88 to 390 nm. This allows us to treat multi photon ionization of argon ranging from one- to five-photon ionization. Laser pulses with durations of 30 optical cycles or less were used in most cases, except for one 60-cycle example to better resolve a predicted resonance structure for a photon energy around 12.75 eV. Although the current problem in Ar is significantly larger than the Ne case treated earlier, by employing our new algorithm, it is still manageable using OpenMP on single-node multiple-core machines. A single laser pulse typically requires a few hours of CPU time on our local cluster. For example, after truncating the energy spectrum at 10 a.u., the matrix sizes were 1618 and 2133 for the ^1S and $^1P^o$ blocks, respectively. Expanding the time-dependent wave function in terms of six *L* blocks (i.e., $L_{max}=5$), as for the cases of two-photon ionization shown below, the rank of the entire matrix (with many zero blocks due to the dipole selection rules), was only 12 263. Even for $L_{max}=9$ (used for five-photon ionization), the rank just exceeded 20 000.

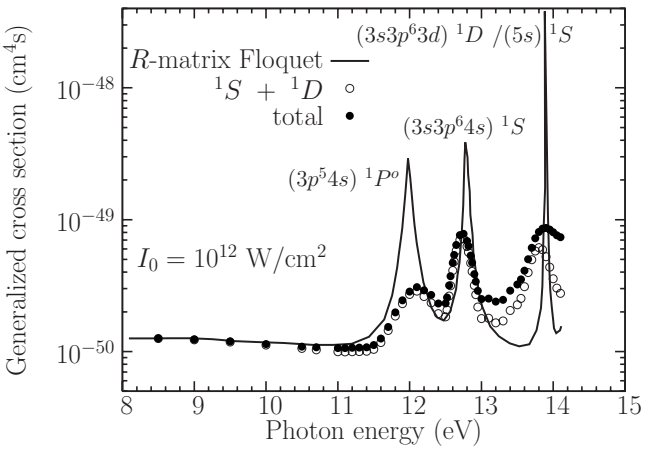

FIG. 1. Generalized cross section for two-photon ionization of $\mathrm{Ar}(3p^6)^1S$ as a function of photon energy. A 30-cycle laser pulse with a peak intensity of 10^{12} W/cm^2 was used in the calculations. The filled circles represent the results obtained by using the total ionization yield, while the open circles show those generated by summing up the partial ionization yields from the individual channels (see the text). The Floquet results are from McKenna and van der Hart [20].

One of the appealing features of the time-dependent algorithm employed in this work is its effectiveness. We only had to use a few hundred (typically about 200) steps per optical cycle, independent of the wavelength. Note that almost 2000 steps per cycle were used in Ref. [14].

III. RESULTS AND DISCUSSION

A. Two-photon ionization

For a sufficiently weak intensity of the laser pulse, for example, $I_0=10^{12}$ W/cm^2 used in much of this work, the ac-Stark shifts of the energy levels are negligible. Given the first ionization potential of 15.7 eV, single ionization of argon is characteristic of the two-photon ionization process for photon energies between 7.85 and 15.7 eV.

Figure 1 shows our results for the generalized two-photon cross section of the argon atom, focused on the photon energy in the region from 8 to 14 eV. The present results were obtained by using a laser pulse with a peak intensity of $I_0=10^{12}$ W/cm^2 and a duration of 30 cycles, including a linear ramp on and ramp off over five cycles. Note that the two-photon cross sections obtained by the present fully time-dependent approach is predicted to exhibit three resonance peaks around photon energies of 12.0, 12.75, and 13.9 eV, respectively. These peaks were also seen by McKenna and van der Hart [20], who employed the *R*-matrix Floquet approach. As mentioned above, this method effectively corresponds to an infinitely long pulse and thus a sharply defined photon energy. Although not shown on the graph, we note that similarly good agreement with the Floquet results for this and other cases was achieved with the independently

developed time-dependent *R*-matrix approach of the Belfast group [14].

In the present TDBSR method, the essential ingredients for extracting the multiphoton ionization cross sections are the ionization yield at the end of the laser pulse and the effective interaction time (T_{eff}). While the role of T_{eff} was highlighted above, a few remarks regarding the ionization yield seem appropriate. At this point, we have two sets of ionization yields at the end of the pulse, namely, (i) the total yield and (ii) the partial ionization yields populated in the relevant ionization channels. For the dominant two-photon process described here, the latter correspond to the ^1S and ^1D final continuum states. At first sight, one might think that both the total and the partial ionization yields can be used to obtain the generalized cross sections. This produces the two sets of results in Fig. 1. Indeed, there are no significant differences for photon energies below ≈13 eV. When the photon energy approaches the threshold for one-photon ionization, however, we observe that the cross section extracted from the total ionization yield is noticeably larger than that obtained from the ^1S and ^1D partial ionization yields. In this case the total ionization yield contains contributions from the $^1P^o$ symmetry, i.e., from the single-photon ionization probability. Note that the generalized cross sections shown below were obtained using the probabilities derived from the dominant symmetries, while the ionization yields include the contributions from all partial waves.

No structure is seen when the photon energy is varied between 8 and 11 eV. However, when the photon energy increases from 11 to 14 eV, several resonance peaks appear. These can be understood by analyzing the eigenvalues of the Hamiltonian. The resonance at 12.0 eV can be attributed to the photon energy coming into resonance, through a single-photon excitation process, with the intermediate excited state $\text{Ar}^*(3p^5 4s)^1P^o$. This is the lowest state in the $^1P^o$ symmetry, with an absolute energy of −526.574 a.u. in our calculation. This corresponds to an excitation energy of 12.01 eV from the neutral initial state, in good agreement with the NIST value of 11.83 eV [19]. The next resonance occurring at a photon energy of 12.75 eV is due to an intermediate-state resonance between an autoionizing state and the ground state through a two-photon absorption process. For the argon atom, autoionizing states converging to the second ionization threshold corresponding to the $\text{Ar}^+(3s3p^6)$ ionic state are the $(3s3p^6n\ell)^1L$ series, which are embedded in the continuum of the $(3s^2 3p^5 k\ell)^1L$ states. Among them, the channels corresponding to $(3s3p^6ns)^1S$ and $(3s3p^6nd)^1D$ are reachable by the absorption of two photons from the ground state $(3s^2 3p^6)^1S$. This is the reason for the resonance at 12.75 eV, when the photon hits the intermediate $(3s3p^6 4s)^1S$ state after two-photon absorption. In some earlier calculations (see, for example, Pan *et al.* [21]), the resonance at 12.75 eV was not seen, since coupling to the $\text{Ar}^+(3s3p^6)$ state was not included.

Returning to the resonance at 12.0 eV, we should also point out a competing process to the two-photon ionization. This can be explained by a simplified two-level model. As mentioned above, the photon energy matches the energy gap between the $(3p^6)^1S$ and $(3p^5 4s)^1P^o$ states very well in this case. Consequently, the excitation probability of the

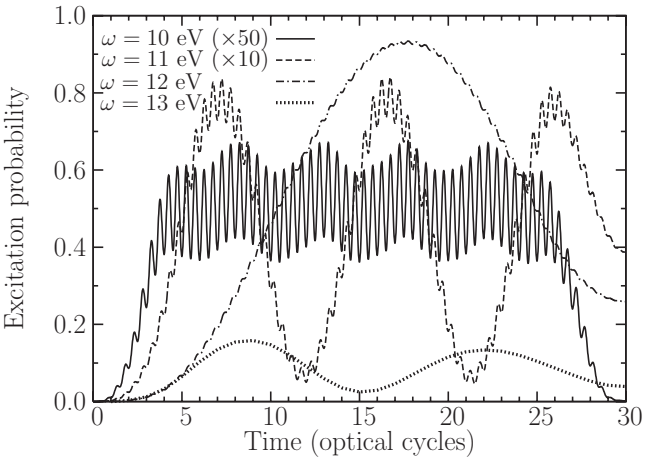

FIG. 2. Excitation probability of argon for a 30-cycle laser pulse with a peak intensity of 2×10^{13} W/cm^2 and photon energies of 10, 11, 12, and 13 eV. Note the different scales for the individual photon energies.

$(3p^5 4s)^1P^o$ state through absorption of the first photon will be large. The electron may now be efficiently ionized by the absorption of a second photon from the $(3p^5 4s)^1P^o$ state. On the other hand, quantum mechanics tells us that there is interference between the ionization and stimulated deexcitation back to the ground state, and thus the entire process is not simply overwhelmed by ionization at the resonance energy.

The above mechanism becomes evident by looking at Fig. 2, which depicts the excitation probability at different photon energies. These so-called Rabi oscillations occur when the photon energy matches the energy gap between the two states, leading to oscillations in the excitation probability with a large amplitude and a long oscillation period. When the photon energy is tuned away from the energy gap, there are still oscillations, but with much smaller amplitudes and shorter Rabi periods. Note that the period of the Rabi oscillation can be estimated as $\mathcal{T}_{\text{R}}(\omega)=\sqrt{(\Delta E)^2+W_{\text{fi}}^2}$, where ΔE

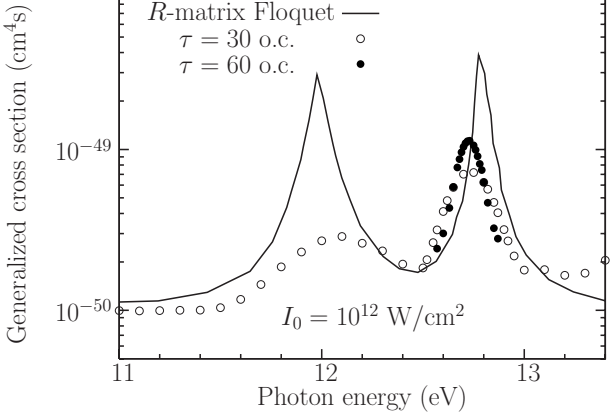

FIG. 3. Effect of the pulse duration on the generalized cross section for two-photon ionization of argon. Laser pulses with durations of 30 or 60 optical cycles and a peak intensity of 10^{12} W/cm^2 were used. The Floquet results are from McKenna and van der Hart [20].

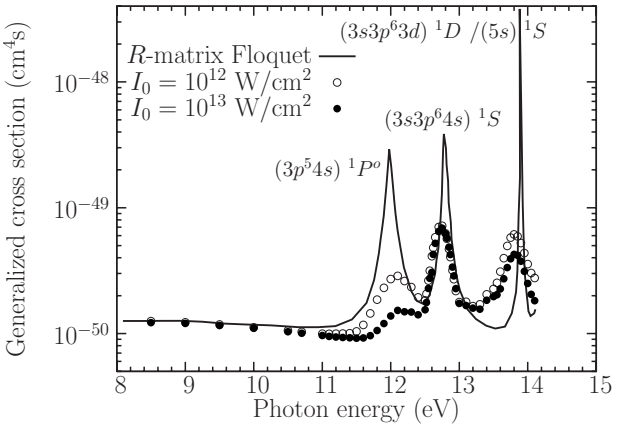

FIG. 4. Effect of the laser peak intensity on the generalized two-photon cross section for a 30-cycle laser pulse. The Floquet results are from McKenna and van der Hart [20].

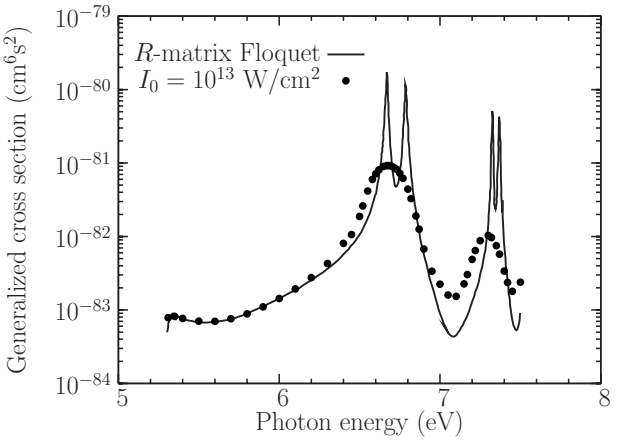

FIG. 5. Generalized cross section for three-photon ionization of argon atoms as a function of photon energy for a 30-cycle laser pulse of peak intensity 10^{13} W/cm^2. The Floquet results are from McKenna and van der Hart [20].

denotes the energy detuning ($\Delta E = \omega - \omega_{\rm fi}$) and $W_{\rm fi}$ is the coupling strength between the two energy levels induced by the external laser field. The amplitude of the Rabi oscillation is approximately given by $\mathcal{A}_{\rm R}(\omega) = W_{\rm fi}^2/[W_{\rm fi}^2 + (\omega - \omega_{\rm fi})^2]$. If the photon energy exactly hits the energy gap, i.e., $\omega = \omega_{\rm fi}$, the system can be completely pumped to the excited state. This is in good agreement with Fig. 2. Since the present *ab initio* calculations also include effects from other states, however, the maximum population is not exactly unity.

Similarly, for a higher photon energy, the photon can also hit the $(3s3p^63d)^1D$ state, thereby resulting in the third resonance peak in Fig. 1 just below a photon energy of 14 eV. The analysis in Ref. [20] suggests that this resonance is actually a mixture of the $(3s3p^63d)^1D$ and $(3s3p^65s)^1S$ states. Hence, these two resonances again correspond to an inner-shell ($3s$) excitation process.

Turning to the question of the effect of the pulse duration on the calculated generalized cross sections, Fig. 1 clearly shows that the present results at the resonance photon energies are lower than the predictions of the R-matrix Floquet calculations. As mentioned before, this is simply due to the fact that the Floquet method corresponds to an infinitely long pulse. This is equivalent to using a single, precise photon energy and therefore no broadening of the resonances occurs. In a fully time-dependent approach, such as the one used in the present work, the system is subjected to a temporal laser field with a limited pulse duration and the cross sections must be extracted from the propagated wave function using indirect techniques subject to a finite energy resolution.

As an example, Fig. 3 shows the effect of the pulse duration on the two-photon ionization cross section around the photon energy of 12.75 eV. As expected, increasing the pulse length to 60 optical cycles (again including a 5-cycle ramp on and ramp off), i.e., making the laser frequency sharper, results in a higher resonance peak with a narrower energy, in closer agreement with the R-matrix Floquet results of McKenna and van der Hart [20]. In addition to the pulse duration, we note that there are other differences between the two sets of calculations. Of particular importance are the different descriptions of both the initial bound state and the final ionic states, as well as the number of coupled states. These differences are responsible for the small shift in the energy position of the resonance in the vicinity of 12.75 eV.

Finally, Fig. 4 shows the effect of the laser intensity on the generalized two-photon cross section. While both peak intensities, 10^{12} and 10^{13} W/cm^2, still lie in the perturbative regime, the height of the first resonance peak is significantly diminished for the more intense laser field.

B. Generalized cross sections for three-photon and five-photon ionization

We now turn to processes needing more than two photons to ionize the argon atom. Specifically, Fig. 5 shows the generalized cross section for three-photon ionization while Fig. 6 depicts our results for the five-photon process. In the latter case, the wavelength ranges between 330 and 390 nm. Once again, our predictions agree in a satisfactory way with the Floquet results of McKenna and van der Hart [20] (three photons) and van der Hart [22] (five photons), bearing in

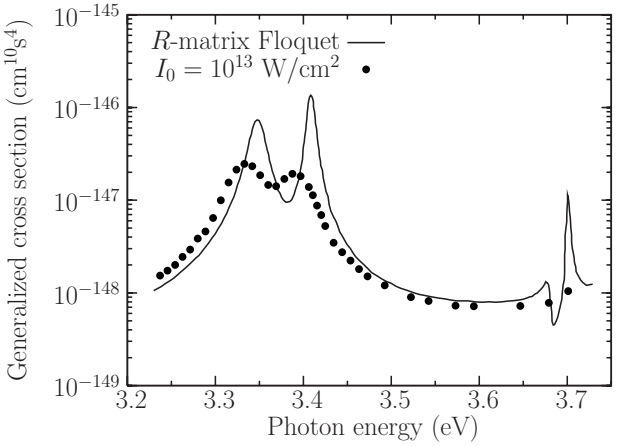

FIG. 6. Generalized cross section for five-photon ionization of argon atoms as a function of photon energy for a 30-cycle laser pulse of peak intensity 10^{13} W/cm^2. The Floquet results are from van der Hart [22].

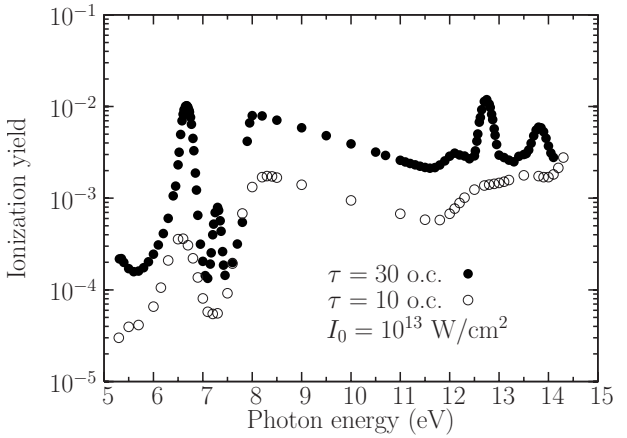

FIG. 7. Ionization yield as a function of photon energy in 10-cyle and 30-cycle laser pulses of peak intensity 10^{13} W/cm^2.

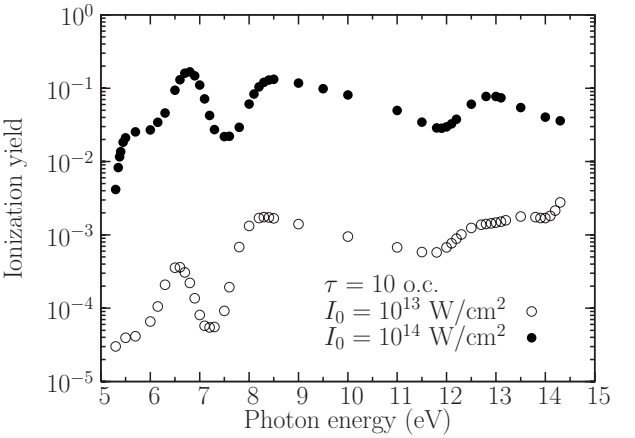

FIG. 8. Ionization yield as a function of photon energy in 10-cycle laser pulses with peak intensities of 10^{13} and 10^{14} W/cm^2.

mind the expected broadening of our features due to the finite duration of the laser pulse and the changes in the resonance positions related to differences in the atomic structure models.

C. Ionization yield for two-photon and three-photon ionization

We finish this section by showing two examples of the ionization yield for photon energies in the regime dominated by two-photon and three-photon processes. Note that, due to the different photon numbers involved, it does not make sense to define a generalized cross section in this case. Figure 7 shows the yield for a fixed peak intensity of 10^{13} W/cm^2 but pulses of different length. In addition to the expected smaller ionization rate for the 10-cycle pulse (for this pulse the ramp on and ramp off were chosen as three cycles each), some of the structures resolved in the 30-cycle pulse completely disappear. This is another example of feature broadening with decreasing pulse length.

Finally, Fig. 8 shows the effect of increasing the laser peak intensity by another order of magnitude, this time for the short 10-cycle pulse. In addition to the larger ionization yield for the more intense pulse, we notice qualitative differences in the energy dependence of the ionization yield, with a significant shift in the low-energy regime. This is a consequence of the large ac-Stark shift for a peak intensity as high as 10^{14} W/cm^2.

IV. CONCLUSIONS AND OUTLOOK

We applied the TDBSR method to multiphoton ionization of argon atoms by a strong short laser pulse. The present calculations became possible via a significant improvement in the numerical implementation of the method. Where applicable, excellent agreement with predictions from *R*-matrix Floquet calculations, as well as those from an independently developed time-dependent *R*-matrix approach has been obtained.

In light of the improvements in the efficiency and stability of our method, we are confident that we are now able to perform accurate multiphoton, single-ionization, and excitation calculations for essentially all atomic targets of current experimental interest. As the next step, we plan to extend the method to allow for two electrons in the continuum and check the results against the wealth of theoretical predictions available for double ionization of helium. Thereafter, we will turn our attention to the double ionization of complex targets, starting again with Ne and Ar, for which experiments are currently under way or in preparation. In these cases, coupling to a singly or doubly ionized core with nonzero angular momentum will significantly increase the size of the matrices we will need to handle. However, we are confident that the TDBSR method, coupled with access to large scale computational resources available at National Science Foundation and U.S. Department of Energy computational facilities, will enable us to tackle these experimentally interesting and highly challenging problems in short-pulse, strong-field atomic physics.

ACKNOWLEDGMENTS

This work was supported by the United States National Science Foundation under Grants No. PHY-0757755 (X.G. and K.B.) and No. PHY-0555226 (C.J.N., O.Z., and K.B.). We gratefully acknowledge supercomputer resources provided by the U.S. Department of Energy through its National Energy Research Scientific Computer Center (NERSC) and the NSF through Teragrid allocations at the Texas Advanced Computing Center (TACC).

[1] X. Guan, O. Zatsarinny, K. Bartschat, B. I. Schneider, J. Feist, and C. J. Noble, Phys. Rev. A **76**, 053411 (2007).
[2] O. Zatsarinny, Comput. Phys. Commun. **174**, 273 (2006).
[3] T. J. Park and J. C. Light, J. Chem. Phys. **85**, 5870 (1986).
[4] B. I. Schneider and L. A. Collins, J. Non-Cryst. Solids **351**, 1551 (2005).
[5] See the KITP Attosecond Science Workshop; http://www.kitp.ucsb.edu/activities/auto2/?id=333.
[6] M. Uiberacker, Th. Uphues, M. Schultze, A. J. Verhoef, V. Yakovlev, M. F. Kling, J. Rauschenberger, N. M. Kabachnik, H. Schröder, M. Lezius, K. L. Kompa, H.-G. Muller, M. J. J. Vrakking, S. Hendel, U. Kleineberg, U. Heinzmann, M. Drescher, and F. Krausz, Nature (London) **446**, 627 (2007).
[7] A. A. Sorokin, M. Wellhöfer, S. V. Bobashev, K. Tiedtke, and M. Richter, Phys. Rev. A **75**, 051402(R) (2007).
[8] R. Moshammer, Y. H. Jiang, L. Foucar, A. Rudenko, Th. Ergler, C. D. Schröter, S. Lüdemann, K. Zrost, D. Fischer, J. Titze, T. Jahnke, M. Schöffler, T. Weber, R. Dörner, T. J. M. Zouros, A. Dorn, T. Ferger, K. U. Kühnel, S. Düsterer, R. Treusch, P. Radcliffe, E. Plönjes, and J. Ullrich, Phys. Rev. Lett. **98**, 203001 (2007).
[9] X. Guan, K. Bartschat, and B. I. Schneider, Phys. Rev. A **77**, 043421 (2008).
[10] J. Feist, S. Nagele, R. Pazourek, E. Persson, B. I. Schneider, L. A. Collins, and J. Burgdörfer, Phys. Rev. A **77**, 043420 (2008).
[11] P. G. Burke, P. Francken, and C. J. Joachain, J. Phys. B **24**, 761 (1991).
[12] M. Plummer and C. J. Noble, J. Phys. B **36**, L219 (2003).
[13] P. G. Burke and V. M. Burke, J. Phys. B **30**, L383 (1997).
[14] H. W. van der Hart, M. A. Lysaght, and P. G. Burke, Phys. Rev. A **76**, 043405 (2007).
[15] G. H. Golub and Q. Ye, SIAM J. Sci. Comput. (USA) **24**, 312 (2002).
[16] K. C. Kulander, K. J. Schafer, and J. L. Krause, in *Atoms in Intense Laser Fields*, supplement to Advanced in Atomic, Molecular, and Optical Physics, edited by M. Gavrila (Academic Press, Inc., San Diego, 1992), p. 247.
[17] P. G. Burke and K. T. Taylor, J. Phys. B **8**, 2620 (1975).
[18] C. Froese Fischer, T. Brage, and P. Jönsson, *Computational Atomic Structure: An MCHF Approach* (Institute of Physics Publishing, Bristol, 1997).
[19] http://physics. nist.gov/PhysRefData/ASD/
[20] C. McKenna and H. W. van der Hart, J. Phys. B **37**, 457 (2004).
[21] C. Pan, B. Gao, and A. F. Starace, Phys. Rev. A **41**, 6271 (1990).
[22] H. W. van der Hart, Phys. Rev. A **73**, 023417 (2006).